

# Influence of Quartz on the Hydration of $3 \text{CaO} \cdot \text{Al}_2\text{O}_3$

H. N. STEIN, Laboratory for Inorganic Chemistry, Technological University, Eindhoven, Netherlands

Quartz is found to intensify the heat evolution peak in  $3 \text{CaO} \cdot \text{Al}_2\text{O}_3$ -water pastes connected with conversion of hexagonal intermediate hydrates into the final products (cubic  $3 \text{CaO} \cdot \text{Al}_2\text{O}_3 \cdot 6 \text{H}_2\text{O}$  and hydrous alumina). Chemical analyses of the liquid phase in suspensions of  $3 \text{CaO} \cdot \text{Al}_2\text{O}_3$  in water in the absence and in the presence of quartz are at variance with a mechanism involving a chemical action of quartz, and indicate that the quartz particles act as precipitation sites for hydrous alumina. Heat evolution data are consistent with an analogous action in pastes.

•WHEN a portland cement paste is hydrating isothermally, a number of heat evolution peaks can be recorded (1). In any heat evolution peak, the rising branch is especially noteworthy, since the descending branch may be readily explained by, e.g., formation of a hydrate layer on the reacting surfaces or exhaustion of the reacting species.

In order to learn more about the fundamental mechanism operating at the stages involving an accelerated heat evolution, phenomena in pastes of pure cement compounds are of interest, since their interpretation is facilitated by the absence of interaction between various constituents of a mixture like portland cement.

In pastes of  $\text{C}_3\text{A}^*$ , two heat evolution peaks are found (2, 3), one starting at the first contact of  $\text{C}_3\text{A}$  with water. The second was shown in a previous investigation (3) to be connected with conversion of intermediate hexagonal hydrates ( $\text{C}_2\text{AH}_6$ ,  $\text{C}_4\text{AH}_{13}$ ) into the final products ( $\text{C}_3\text{AH}_6$  and hydrous alumina); the principal argument was the influence of addition of  $\text{C}_3\text{AH}_6$  to the pastes, shifting the second peak to earlier times without notably intensifying it. However, an apparently inert additive like quartz was also observed to influence the second heat evolution peak, though in a different way: the peak was intensified but only slightly shifted to earlier times.

This influence seems to be of interest since quartz is a constituent of nearly all aggregates employed in cement utilization. A highly active form of silica (aerosil) is known to influence  $\text{C}_3\text{S}$  hydration through chemical action (4); the question arises whether the action of quartz might be explained along similar lines, e.g., through  $\text{Ca}^{++}$  adsorption.

## EXPERIMENTAL

### Materials

$\text{C}_3\text{A}$  was synthesized as described in an earlier report (5). Two batches were used, one of them (batch A) prepared from reagent grade (Merck) chemicals as starting materials, the other (batch B) from specpure (Johnson Matthey Ltd.) ingredients. Analyses indicated the presence of the impurities listed in Table 1. The free  $\text{CaO}$  content (6) of all batches was 0.1 percent or less; their X-ray powder diffraction patterns agreed completely with the data mentioned by Taylor (7). They were ground to samples of different specific surfaces in an agate ball mill; the specific surface of a sample, determined by air permeability (8), is mentioned with the individual experiments.

\*Throughout this paper, the abbreviated cement chemical nomenclature is employed:

$\text{C}_3\text{AH}_6 = 3 \text{CaO} \cdot \text{Al}_2\text{O}_3 \cdot 6 \text{H}_2\text{O}$ , etc. Hydrous alumina is a designation for all phases containing (in addition to aluminium, oxygen and hydroxyl ions) only minor amounts of other metal ions.  $\text{C}_4\text{AH}_{13}$  is the  $\alpha$ -tetracalcium aluminate 13-hydrate containing some essential  $\text{CO}_3^{--}$  (7).

TABLE 1  
IMPURITIES PRESENT IN C<sub>3</sub>A  
USED IN EXPERIMENTS  
(Percent by Weight)

Impurity	Batch A	Batch B
Na	0.3 (7)	absent (<0.07)
Mo	0.1	0.07
Mg	0.03	0.006
Si	0.03	0.02
Ti	0.02 (5)	—
Fe	0.01 (4)	0.01
Ga	0.004 (5)	absent (<0.001) (5)
Mn	0.004 (5)	absent (<0.0008)

experiments, twice distilled water was used. All water had been boiled and cooled shortly prior to use.

Nitrogen was purified by passage successively through a washing bottle filled with about 4 N H<sub>2</sub>SO<sub>4</sub>, an absorption tube filled with 13-20 mesh carbosorb, two washing bottles filled with 20 percent NaOH solution and a washing bottle filled with water.

### Methods

Heat evolution rate measurements were performed by isothermal calorimetry (9). Pastes were mixed by grinding solids and liquid in the appropriate ratio in a porcelain dish with a porcelain pestle, in order to disperse aggregates (5). Solid components of a paste were mixed dry by shaking prior to the addition of water.

Conductivity measurements were performed by the method employed in earlier research (4). Care was taken that the magnetic stirrer swept the whole bottom of the thermostated beaker (with the exception of a rim of about 1 mm width), so as to avoid "dead spots" in stirring and to prevent settling of the suspended solids. When starting a conductivity experiment, quartz was added first, then water was pipetted into the beaker. Immediately afterward the beaker was covered and purified nitrogen was passed over the suspension, the nitrogen exit being protected against backflow of air by a carbosorb-filled tube. Stirring was started, and C<sub>3</sub>A was added through a small hole in the cover that was closed immediately afterward by a rubber stopper.

Chemical analysis of the water phase in suspension experiments began with separation of liquid and solids by centrifugation in rubber-stopped tubes (10 min at 4800 rpm), followed immediately by filtration (with suction) of the supernatant liquid through a Schott 1 G 4 sintered glass funnel. During filtration, purified nitrogen was passed over the suspension. Transfer to the centrifugation tubes took 4-5 sec. Samples of the filtrate were pipetted for analysis immediately after filtration. Calcium was titrated in one sample with EDTA after acidification, addition of 5 ml of a 1:1 triethanolamine-water mixture, dilution to about 200 ml and addition of 10 ml 4 N KOH solution with murexide as indicator; aluminum was determined gravimetrically with 8-hydroxyquinoline (10) in a second sample.

In some cases, filtration directly from the thermostated beaker was tried, the suspension being protected against contact with air. Filtration was sluggish, however, supplying only small samples of the solution for analysis, causing great errors in the determinations, although the general line of the results was not significantly different from that of centrifuged samples.

X-ray powder diffraction patterns were determined from solids precipitated during centrifugation (10 min at 4800 rpm). The solids were transferred to a diffractometer sample holder, excess liquid being sucked away with filter paper. Although with this method there is danger of CO<sub>2</sub> action before and during the diffraction experiment, it was considered the best way to obtain data on the solids present at a particular reaction stage. Diffraction patterns were obtained by means of a Philips diffractometer, using CuK $\alpha$ <sub>1</sub> radiation filtered through nickel.

The presence of  $\alpha_1$ -C<sub>2</sub>AH<sub>3</sub> was established by its 10.7 Å and 3.58 spacings, the latter being stronger than is to be expected for C<sub>4</sub>AH<sub>19</sub> (7); in the presence of  $\alpha_1$ -C<sub>2</sub>AH<sub>3</sub>,

Quartz (Riedel de Haen) was heated to 900 C for at least one hour, shortly prior to use. On treating with HF and H<sub>2</sub>SO<sub>4</sub> 0.6 percent residue was left. Its air permeability specific surface was 6.3 x 10<sup>3</sup> cm<sup>2</sup>/g. Its X-ray diffraction pattern agreed completely with the one mentioned by Taylor (7).

Water, demineralized by passage through a column containing a mixture of ion exchange resins (Imac C. 12 and Amberlite IRA 401), was employed in the suspension experiments. For the paste

the additional presence or absence of  $C_4AH_{19}$  is difficult to establish unambiguously. Therefore the statement of the presence of  $\alpha_1-C_2AH_8$  will mean the inclusion of possible additional amounts of  $C_4AH_{19}$ .

Electron microscope investigations were conducted as follows. About 0.5 ml of a suspension was mixed (by shaking) with 10 ml of absolute ethanol (reagent grade, Merck). A drop of the ethanol suspension thus obtained was placed on a carbon-covered copper grid in the usual manner, and left drying in the laboratory air. The electron microscope used was a Philips 75 B.

Temperature conditions for all hydration reactions were  $25 \pm 0.1$  C.

## RESULTS AND DISCUSSION

### Reaction in Suspension

Figure 1 compares two typical experiments on conductivity of suspensions, in the absence and in the presence of quartz, respectively; the early stages are plotted in more detail in Figure 2. In Figure 1, different reaction stages have been designated by letters.

Similar experiments on  $C_3A$  suspensions without quartz have been reported by Segalova et al. (11); these authors interpret their data by assuming that at the more or less constant conductivity level obtained after about 2 hours (stage A, Fig. 1) the metastable solubility of  $C_3A$  is reached.

Chemical analyses of the water phase at stage A showed its composition to lie close to the intersection point of the metastable solubility curves of  $C_2AH_8$  and  $C_4AH_{19}$  in the Jones and Roberts phase diagram for the ternary system  $CaO-Al_2O_3-H_2O$  (12, 13). (Segalova et al. report higher values for  $CaO$  and  $Al_2O_3$  concentrations after addition of lignosulfonate; it remains doubtful, however, whether the action of the lignosulfonate is restricted to regulating crystal size of the hexagonal hydrates, as supposed by these authors, and does not include, e.g., a precipitation of hydrous alumina particles too small to be removed by filtration.) Consistent with these data is the form of the conductivity curve (Fig. 1), showing, in addition to a pronounced peak after 1-2 minutes' hydration, a slight but persistently reproduced effect (indicated by an arrow in Fig. 1) before stage A is reached: it seems reasonable to suppose that both effects are connected with incipient precipitation of one particular hexagonal hydrate. X-ray analyses show the solids at this stage to consist predominantly of  $\alpha-C_2AH_8$  and " $C_4AH_{13}$ " with a small amount of  $C_3A$ , with possibly  $C_4AH_{19}$  present ( $C_3AH_6$  not detectable). It remains unclear whether the " $C_4AH_{13}$ " is formed in the suspension from traces of  $CO_2$  that may be present in spite of all precautions, or during preparation and handling of the diffractometer samples.\*

The simplest way to understand these facts seems to be that, as soon as both  $C_2AH_8$  and  $C_4AH_{19}$  (or " $C_4AH_{13}$ ") are precipitated, the concentrations in the water phase adjust themselves until the invariant point of metastable coexistence of  $C_2AH_8$  and  $C_4AH_{19}$  with solution is reached.

At stage B, X-ray analysis again shows  $\alpha-C_2AH_8$  and " $C_4AH_{13}$ " to be the predominant solid phases present;  $C_3A$  can no longer be detected with certainty; traces of  $C_3AH_6$  are found. Electron micrographs show, in addition to hexagonal particles, a few typical  $C_3AH_6$  crystals (Fig. 4). The concentrations of both " $CaO$ " and " $Al_2O_3$ " in the water phase differ only slightly from the respective values at A (Fig. 3).

---

\*After this paper had been completed, the following experiment was conducted, showing that in the experiments reported in this paper the " $C_4AH_{13}$ " is probably not formed in the suspension. A suspension of  $C_3A$  in  $H_2O$  was prepared using the same precautions against contact with air. After 2 hr hydration, the suspension was filtered with suction (through a Schott IG3 sintered glass funnel) and washed with alcohol and ether or acetone, being protected against contact with air during filtration and washings. A sample of the precipitate was immediately afterward confined in a Lindemann glass capillary closed at one end. One day afterward the diffraction lines of " $C_4AH_{13}$ " were not seen. After two days, however, apparently some  $CO_2$  had been able to penetrate into the capillary; the strongest line of " $C_4AH_{13}$ " ( $d = 8.2$  Å) was observed.

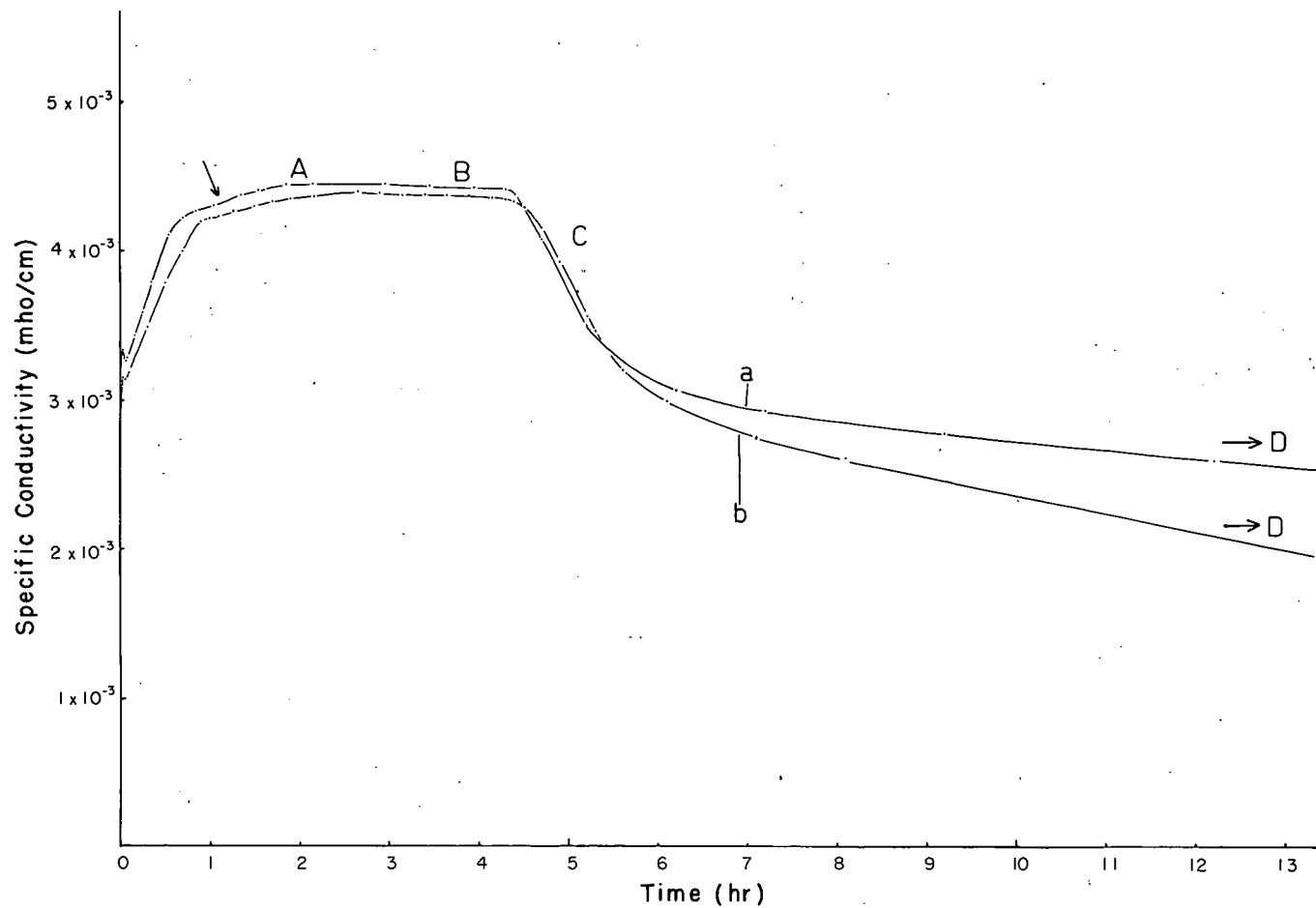


Figure 1. Electrical conductivity vs time for suspensions of  $C_3A$  (+ quartz) + water.  $C_3A$ : batch A, surface area  $6.9 \times 10^2 \text{ cm}^2/\text{g}$ . Curve a: 0.5975 g  $C_3A$  + 60 ml water. Curve b: 0.5985 g  $C_3A$  + 2.9986 g quartz + 60 ml water. Letters A, B, C, D and D' designate different reaction stages.

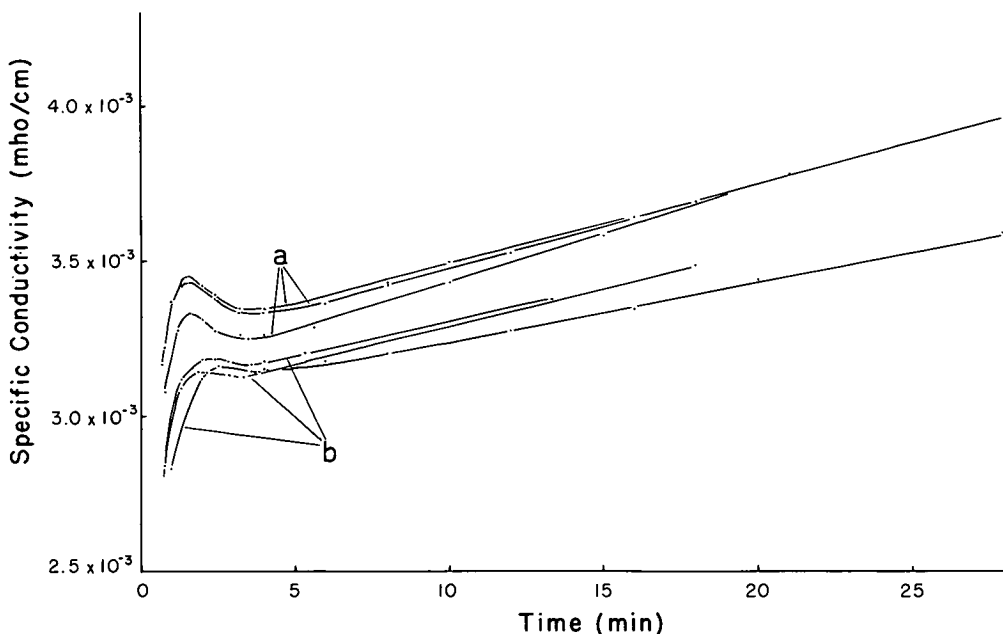


Figure 2. Early stages of the reaction of  $C_3A$  in suspension as followed by electrical conductivity.  $C_3A$ : batch A, surface area  $6.9 \times 10^2 \text{ cm}^2/\text{g}$ . Curves a: 0.60 g  $C_3A$  + 60 ml water. Curves b: 0.60 g  $C_3A$  + 3.00 g quartz + 60 ml water.

Stage C is related to a pronounced decrease in conductivity, slowing down until, after  $16\frac{1}{2}$  hr, stage D is reached. By this time,  $C_3AH_6$  and some " $C_4AH_{13}$ " are the sole solids found by X-rays. The concentrations in the water phase follow the path depicted in Figure 3: the  $Ca^{++}$  ion concentration decreases, the aluminate ion concentration increases. Apparently, by continued precipitation of  $C_3AH_6$  the solution becomes less saturated toward  $C_2AH_8$  and  $C_4AH_{13}$ ;  $C_2AH_8$  is dissolved more rapidly, as evidenced both by the concentration path of the solution and by the greater persistence of " $C_4AH_{13}$ " according to X-ray data.

Somehow, the conversion comes more or less to a standstill at stage D in a region of the phase diagram where precipitation of an amorphous type of hydrous alumina is expected (Fig. 3). The most probable hypothesis is that alumina, being precipitated preferentially on a surface, covers the  $C_3AH_6$  nuclei (the motors of the conversion of the intermediates into the stable products), inactivates them and thus stops the reaction. It will be noted that at stage D the solubility curve of highly unstable alumina gel (according to the Jones and Roberts phase diagram) is not yet reached. However, the solubility of hydrous alumina strongly depends on its crystallinity; its precipitation in the region concerned has been observed (12, 13).

Consistent with the ideas expressed are electron micrographs which show a rapid increase in  $C_3AH_6$  particles at stage C (Fig. 5) and predominantly  $C_3AH_6$  particles at stage D (Fig. 6). Some bodies are seen between the  $C_3AH_6$  particles in the latter figure, among which are hexagonal ones, others being less distinctly crystalline and thus possibly amorphous hydrous alumina. Evidence of the latter, however, is not pronounced; if it is precipitated on the  $C_3AH_6$  nuclei, as supposed, it is not expected to be very clearly seen.

The influence of quartz on the conductivity vs time curve may be summarized as follows:

1. The supersaturation needed for crystallization of the first calcium aluminate hydrate to be precipitated is depressed (Fig. 2). The quartz surfaces apparently act as precipitation sites.

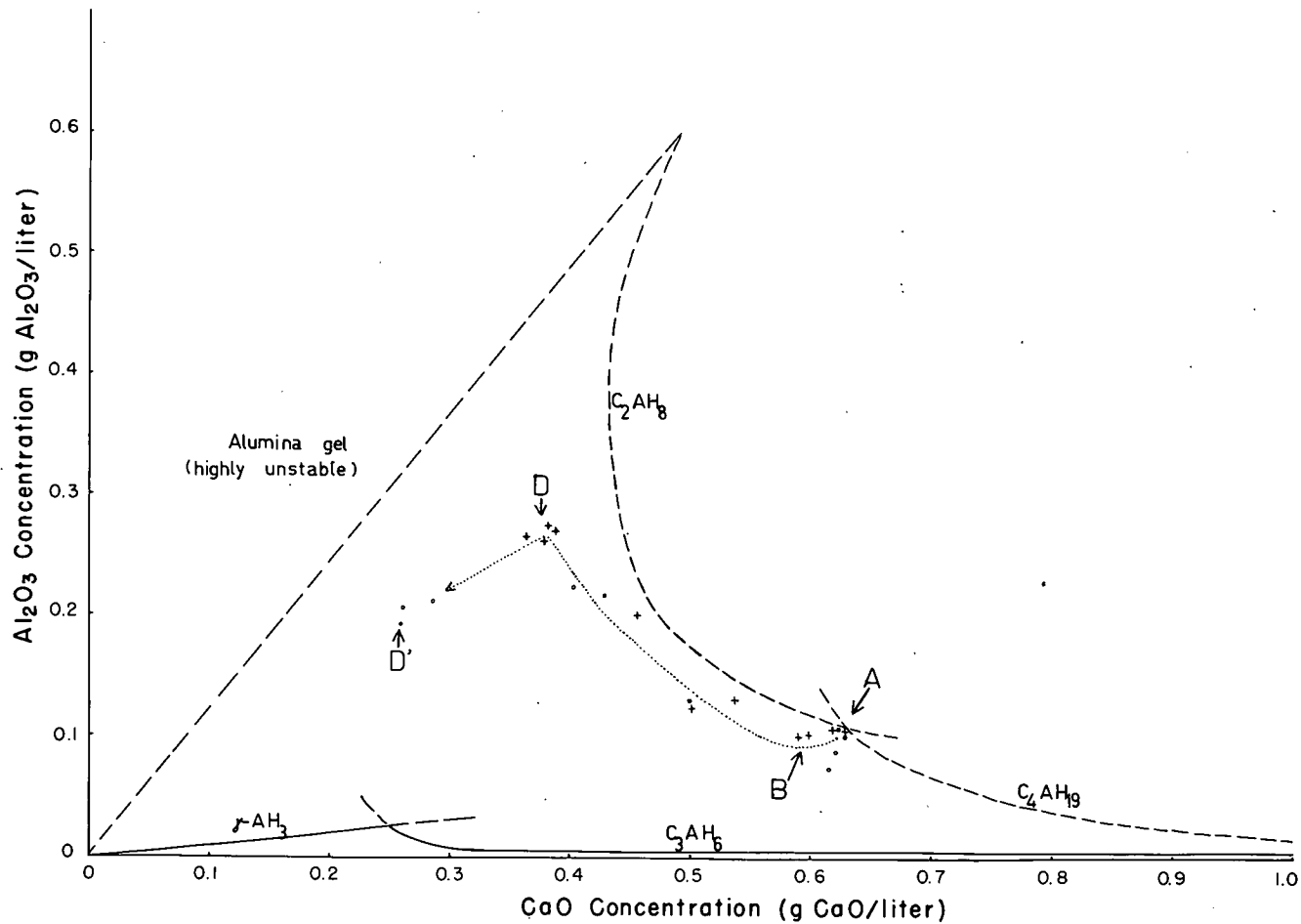


Figure 3. Concentration relations in the water phase of suspensions  $C_3A$  (+ quartz) + water.  $C_3A$ : batch A, surface area ranging from  $6.9 \times 10^2$  to  $7.5 \times 10^2$   $cm^2/g$ .  $+ -0.60$  g  $C_3A$  +  $60$  ml water.  $o - 0.60$  g  $C_3A$  +  $3.00$  g quartz +  $60$  ml water. Dotted line shows concentration path during crystallization of  $C_3AH_6$ . Letters indicate reaction stages as in Figure 1.

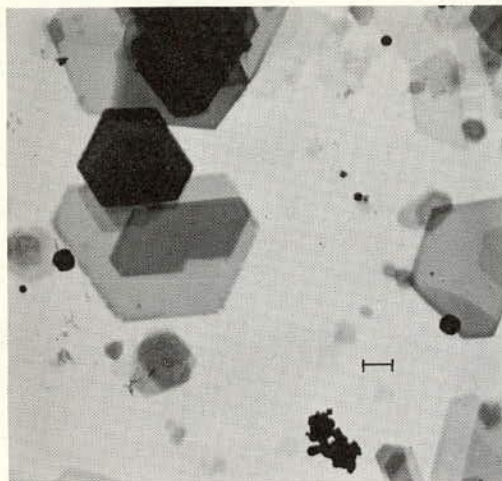


Figure 4. Electron micrograph of a suspension of  $C_3A$  in water at stage B.  $C_3A$ : batch A, surface area  $6.9 \times 10^2 \text{ cm}^2/\text{g}$ , 0.5948 g  $C_3A$  in 60 ml water, 4 hr after the start of hydration. The bar represents  $1 \mu$ .

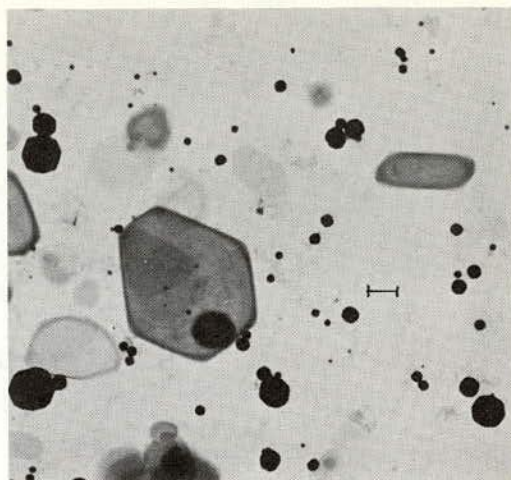


Figure 5. Electron micrograph of a suspension of  $C_3A$  in water at stage C.  $C_3A$ : batch A, surface area  $6.9 \times 10^2 \text{ cm}^2/\text{g}$ , 0.5948 g  $C_3A$  in water, 5.40 hr after the start of hydration. The bar represents  $1 \mu$ .

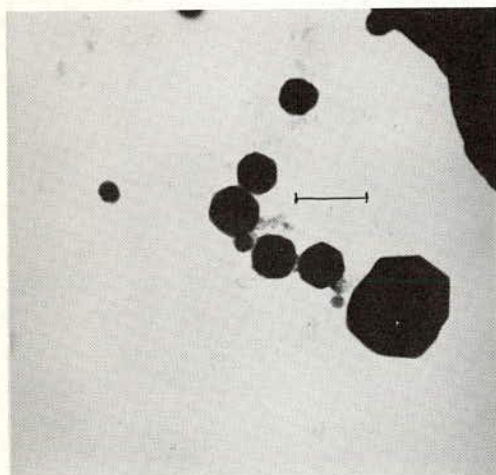


Figure 6. Electron micrograph of a suspension of  $C_3A$  in water at stage D.  $C_3A$ : batch A, surface area  $6.9 \times 10^2 \text{ cm}^2/\text{g}$ , 0.5955 g  $C_3A$  in 60 ml water, 16.20 hr after the start of hydration. The bar represents  $1 \mu$ .

lution in the presence of quartz, inactivates the  $C_3AH_6$  nuclei to a much smaller extent than in the absence of quartz, because it is precipitated partially on the quartz surfaces. The conversion of the hexagonal hydrates into the cubic  $C_3AH_6$  continues; since, however, in addition to  $C_3AH_6$  there is also precipitated hydrous alumina, the concentration path turns towards the origin (Fig. 3).

2. There is no distinct effect on the calcium and aluminate concentrations in the water phase at stage A (Fig. 3). The decreased conductivity of the quartz-containing suspensions as compared with that of quartz-free ones (Figs. 1, 2) may be reasonably explained by the higher solid content. The absence of an influence of quartz on the composition of the water phase at stage A is consistent with the interpretation of its being close to the invariant point of metastable coexistence of  $C_2AH_8$  and  $C_4AH_{19}$  with solution.

3. There is no distinct effect on the course of the reaction during the early stage C, either on the concentration path followed (Fig. 3) or on the rate of concentration change (Fig. 1), or on the time of onset of stage C. Thus, in suspensions any significant effect of quartz on the nucleation of  $C_3AH_6$  appears to be absent.

4. Ultimately, a lower conductivity and a different place in the concentration diagram is reached (stage D'). The following explanation seems reasonable: hydrous alumina, when precipitating from the so-

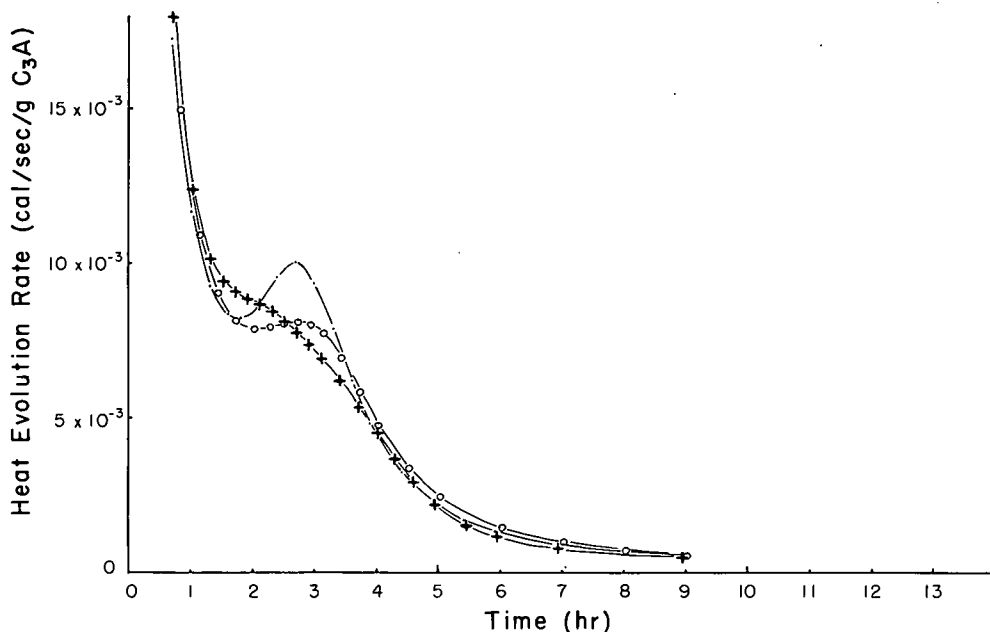


Figure 7. Influence of quartz on heat evolution characteristics of  $C_3A$  + water pastes.  $C_3A$ : batch B, surface area  $16.3 \times 10^2 \text{ cm}^2/\text{g}$ . +—0.9991 g  $C_3A$  + 1.000 g water. o—1.0004 g  $C_3A$  + 0.1228 g quartz + 1.000 g water. ·—0.9985 g  $C_3A$  + 0.3747 g quartz + 1.000 g water.

### Results on Pastes

Heat evolution data, obtained on pastes of  $C_3A$  + water in the absence and in the presence of quartz, follow essentially the same line as found in earlier work (3) (Fig. 7). Attention is drawn to the following points:

1. In this investigation,  $C_3A$  prepared from specpure ingredients was used. The fact that phenomena in these pastes are analogous to those found with  $C_3A$  of a higher impurity level (consistent with the Jones and Roberts phase diagram) indicates that small amounts of impurities do not noticeably change the equilibrium conditions, as suggested by Crowley (14).

2. Influence of changing settling characteristics is investigated through comparing pastes with different  $H_2O/C_3A$  ratios. Figure 8 shows some duplicate experiments illustrating the reproducibility of the heat liberation curves. At lower water content of the pastes, the second peak is seen to shift to earlier times, analogous to the influence of  $C_3AH_6$  addition (3). It appears (as, indeed, might have been anticipated) that at lower water content there is more chance for high local calcium and aluminum ion concentrations favoring  $C_3AH_6$  nucleus formation. The totally different action of quartz shows that its effect is not due to changing settling conditions.

When interpreting the paste results with the aid of suspension experiments, care must be exercised since, in pastes, unhydrated  $C_3A$  is known to persist beyond the second peak, i.e., when considerable amounts of  $C_3AH_6$  are present, in contrast with the situation observed in suspensions. It should be noted, however, that the mechanism of quartz particles acting as precipitation sites for hydrous alumina, guarding both  $C_3AH_6$  nuclei and  $C_3A$  surfaces from being covered, certainly is consistent with the data. The number of  $C_3AH_6$  nuclei present is not significantly changed by quartz, as evidenced by its scarcely influencing the time of appearance of the second peak, nor is the precipitation situation for hydrous alumina noticeably



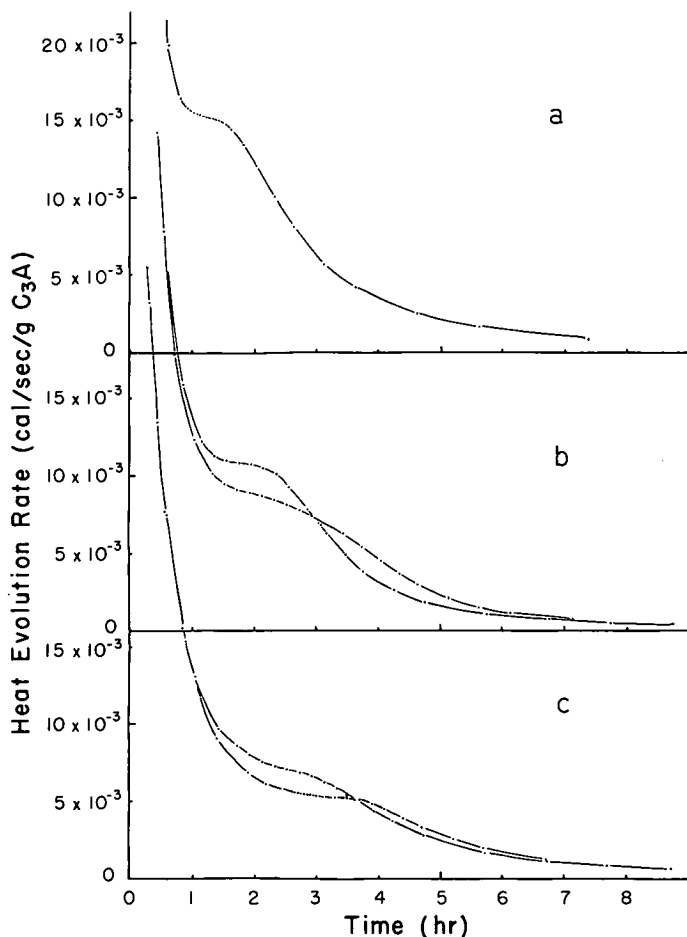


Figure 8. Influence of changing  $\text{H}_2\text{O}/\text{C}_3\text{A}$  ratio on heat evolution characteristics of  $\text{C}_3\text{A}$  + water pastes: a— $\text{H}_2\text{O}/\text{C}_3\text{A} = 0.70$ ; b— $\text{H}_2\text{O}/\text{C}_3\text{A} = 1.00$ ; c— $\text{H}_2\text{O}/\text{C}_3\text{A} = 2.00$ .

influenced by changes in  $\text{H}_2\text{O}/\text{C}_3\text{A}$  ratio or by the addition of  $\text{C}_3\text{AH}_6$  nuclei; the slope of the heat evolution curve during the second peak is not distinctly changed by variations in  $\text{H}_2\text{O}/\text{C}_3\text{A}$  ratio or in amount of  $\text{C}_3\text{AH}_6$  added.

A similar action is found to occur in pastes of  $\text{C}_3\text{A} + \text{CaSO}_4 \cdot 2 \text{ aq} + \text{quartz} + \text{water}$ ; in this case the ettringite particles act as precipitation sites (15).

### CONCLUSIONS

Results of research on the chemical composition of the water phase in  $\text{C}_3\text{A}$  suspensions in the absence and in the presence of quartz, respectively, are at variance with a mechanism involving a chemical action of quartz through, e.g.,  $\text{Ca}^{++}$  adsorption. Although a slight effect on nucleation of the hexagonal intermediate hydrates is found, the solution adjusts itself after some hours to a composition corresponding to the invariant point of metastable coexistence of  $\text{C}_2\text{AH}_8$  and  $\text{C}_4\text{AH}_{19}$  with solution, whether quartz is present or not. The results are consistent with the hypothesis of the quartz particles acting as precipitation sites for hydrous alumina, enabling the  $\text{C}_3\text{AH}_6$  crystals to continue their role as nuclei more effectively.

Paste hydration data agree with the quartz acting in pastes in a similar way.

## ACKNOWLEDGMENTS

The author expresses his gratitude to Prof. Dr. J. M. Stevels for his continued interest in this investigation, to Dr. N. W. H. Addink of Philips Research Laboratories, Eindhoven, for conducting the  $C_3A$  analyses, to Miss F. A. G. M. van Elderen and Miss M. Coppelmans for assistance in the analytical part of the work, and to Miss Y. Leeuwenburgh for carrying out the X-ray analyses.

## REFERENCES

1. Lerch, W. Proc. ASTM, Vol. 46, p. 1252, 1946.
2. Calvet, E., and Longuet, P. Comptes Rendus du 27me Congrès Int. de Chimie Industrielle, Bruxelles, 1954. Vol. 3, p. 31; Chem. Abstr., Vol. 50, p. 9131 a, 1954.
3. Stein, H. N. Jour. Appl. Chem., Vol. 13, p. 228, 1963.
4. Stein, H. N., and Stevels, J. M. Jour. Appl. Chem., Vol. 14, p. 338, 1964.
5. Stein, H. N. Rec. Trav. Chim. Pays-Bas, Vol. 81, p. 881, 1962.
6. Pressler, E. E., Brunauer, S., and Kantro, D. L. Analyt. Chem., Vol. 28, p. 896, 1956.
7. Taylor, H. F. W. In: The Chemistry of Cements, H. F. W. Taylor, ed. Vol. 2, p. 347. Academic Press, London and New York, 1964.
8. Lea, F. M. The Chemistry of Cement and Concrete, revised ed., p. 327. Edward Arnold Ltd., London, 1956.
9. Stein, H. N. Jour. Appl. Chem., Vol. 11, p. 474, 1961.
10. Fresenius, R., and Jander, G. Handbuch der analytischen Chemie. III. Teil, Band 3, p. 258, Berlin, 1942.
11. Segalova, E. E., Solov'eva, E. S., and Rebinder, P. A. Doklady Akad. Nauk SSSR, Vol. 117, p. 841, 1957.
12. Jones, F. E., and Roberts, M. H. Building Research Current Papers, Research Series 1, June 1962.
13. Turriziani, R. The Chemistry of Cements, H. F. W. Taylor, ed. Vol. 1, p. 248. Academic Press, London and New York, 1964.
14. Crowley, M. S. Jour. Amer. Ceramic Soc., Vol. 47, p. 144, 1964.
15. Stein, H. N. To be published.